Geochemical Journal, Vol. 47, pp. 625 to 638, 2013 doi:10.2343/geochemj.2.0293

Chemical characteristics and $\delta^{34}S$–SO_4^{2-} of acid rain: Anthropogenic sulfate deposition and its impacts on CO_2 consumption in the rural karst area of southwest China

HU DING, YUN-CHAO LANG, CONG-QIANG LIU* and TAO-ZE LIU

State Key Laboratory of Environmental Geochemistry, Institute of Geochemistry, Chinese Academy of Sciences, 46th Guanshui Road, Guiyang 550002, China

(*Received March 25, 2013; Accepted November 6, 2013*)

We analyzed rainwater collected from Huanjiang, China, between June, 2007 and May, 2008, with the aim of understanding the origin of the acid rain and its potential impacts on CO_2 uptake by carbonate weathering in the rural areas of southwest China. The pH of the samples varied between 4.2 and 6.2, with a volume-weighted mean (VWM) of 5.1. The rainwater was characterized by high concentrations of SO_4^{2-}, Ca^{2+}, NH_4^+, and Mg^{2+}. The Na^+ and Cl^-, Ca^{2+} and Mg^{2+}, and SO_4^{2-} and NO_3^- were mainly derived from sea salt, the Earth's crust, and anthropogenic sources respectively. The $\delta^{34}S$–SO_4^{2-} of the rain ranged from –5.6 to –11.0‰, with a mean value of –8.4‰, suggesting that local combustion of coal was the main source of acid rain in the region and that the effect of vehicle emissions could be disregarded. Grouping precipitation events by their air mass back-trajectories showed that anthropogenic sources of SO_4^{2-} and NO_3^- might vary depending on air mass origin and passes. The involvement of sulfuric acid in carbonate weathering at the study site resulted in an increase in weathering rates of about 6.5% and a decrease in CO_2 consumption rates by 13.8%. Further, we estimated that anthropogenic sulfate in the atmosphere, mainly from coal combustion, can cause a decrease in CO_2 consumption rates of up to 9.6% in the study area. The data available at present indicate that even in rural karst regions of southwest China, involvement of anthropogenically derived sulfate can significantly decrease the carbon uptake rate of carbonate weathering.

Keywords: karst, rainwater, chemical composition, carbonate weathering, southwest China

INTRODUCTION

Acid deposition, primarily caused by the precursors of strong acids such as H_2SO_4 and HNO_3, derived from the combustion of fossil fuels, has been a major environmental problem in many urban and rural areas worldwide (Bricker and Rice, 1993). Trends of increasing SO_2 and NO_x emission, associated with increasing energy use, coal combustion, and economic growth in China, have intensified the acid rain problem (Larssen *et al*., 2006). Southwestern China is a region seriously affected by the problems of acid deposition; therefore, the rainwater chemistry of this area has been intensely studied (Han and Liu, 2006; Han *et al*., 2010; Lei *et al*., 1997; Wu *et al*., 2012; Zhang *et al*., 2011). However, as with other studies across China (Huang *et al*., 2009; Xu and Han, 2009), these rainwater chemistry analyses have mainly focused on densely populated urban areas (Aas *et al*., 2007; Han and Liu, 2006; Lei *et al*., 1997; Xiao and Liu, 2002; Zhao and Liu, 2010), with few in remote (Han *et al*., 2010) or rural areas (Wu *et al*., 2012) with little human activity. It has been reported that the rainwater chemistry of remote and rural areas had been seriously influenced by anthropogenic sources in nearby large cities (Wu *et al*., 2012), as most air pollutants have the potential to be transported far from their emission source (Toyama *et al*., 2007; Zhang and Liu, 2004). As the karst region of southwest China, which is currently one of the most deprived districts in the country, undergoes fast-paced urbanization, the negative effects of air pollution would be increasingly seen in suburban and rural areas. Consequently, the impacts of acid deposition on natural geo-ecosystems will increase. A more integrated analytical approach that includes karstic rural sites is therefore required to address the acid deposition occurs because of urbanization (Han *et al*., 2010; Wu *et al*., 2012). Moreover, a study of atmospheric deposition in rural locations can contribute to an understanding of the influences of anthropogenic acid deposition (such as sulfuric acid) on natural geological and ecological processes including carbonate weathering. Sulfuric acid as a weathering agent has been recently recognized as not only enhancing the rate of weathering, but also lowering CO_2 consumption rates (Han and Liu, 2004; Li *et al*., 2008; Liu, 2007). However, the impact of acid

*Corresponding author (e-mail: liucongqiang@vip.skleg.cn)

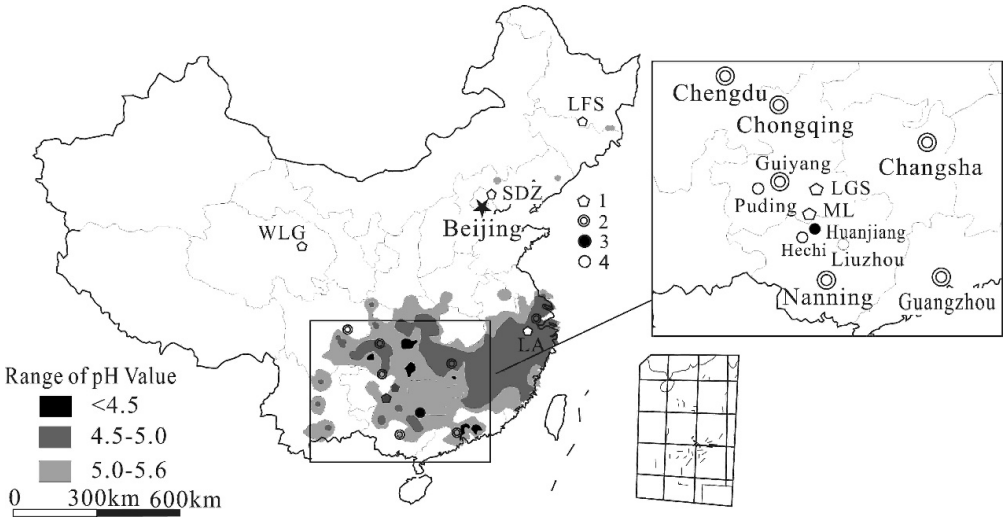

Fig. 1. Sketch map showing Huanjiang and the sampling site as well as the acid rain distribution in China in 2007 (State Environmental Protection Administration of China, 2008). Marker 1 represents the atmosphere background station of China: WLG, LFS, LA and SDZ stand for Waliguan of Qinghai, Longfengshan, Linan and Shangdianzi, which were designed to measure the background values for Northwest, Northeast, North and economically developed Yangtze River Delta of China, respectively (Aas et al., 2007; Li et al., 2010). LGS (IMPACTS, 2004). ML (Han et al., 2010) represents Leigongshan and Maolan of Guizhou Province, which are taken as the background value of southwestern China. Marker 2 shows the capital cities nearby the study site. Marker 3 is the study site. Marker 4 shows the control locations near the study site.

deposition on carbonate weathering is still poorly understood, with most studies mainly focusing on large rivers that generally involve a number of processes and often provide an average of the processes and concentrations from various contributing factors, including rock type, vegetation, meteorology, and land use. No previous studies have yet focused on the influence of acid deposition on carbonate weathering in rural areas. According to Tang (2011), the flux of dust deposition is insignificant in this region of southwest China, because of the abundant rainfall and great distance from the desert; the atmospheric deposition mainly occurs in the form of precipitation. Therefore, we sampled and analyzed the chemical and $\delta^{34}S$–SO_4^{2-} composition of rainwater at a rural site at Huanjiang County, Guangxi Province, a county located in the central karst region of southwest China, in order to (1) gain an initial understanding of the chemical characteristics and variations of atmospheric deposition; (2) identify the possible sources of the various components of wet deposition; and (3) to evaluate the impact of acid deposition on carbonate weathering processes in the karstic rural areas of southwest China.

Sampling and Analysis

Study area

The study site is situated in Huanjiang County, Guangxi, China, and is located in the central part of the Chongqinge–Guiyange–Liuzhou acid rain control zone (Hao *et al*., 2001) (Fig. 1). Huanjiang County is adjacent to Maolan National Reserve, and is approximately 230 km away from the provincial capital Nanning; it has a forest coverage of 69.9%. Huanjiang is one of the most productive agricultural regions in Guangxi, with an agricultural working population of about 320,000, which accounts for around 86% of the total population (Hechi City Government, 2010). There is almost no industrial activity around the study site. Human activities are largely agricultural and include plowing, fertilizing, crop-dusting, amongst others. There is only one city, Hechi, located within 50 km of Huanjiang County. The study area is covered with a typical peak cluster karst landscape. A subtropical mountainous monsoon climate predominates, with a mean annual air temperature of 18.5°C and a mean annual precipitation of 1389 mm, 70% of which falls during the wet season, which lasts from April to the end of August.

Sampling and analysis

The rainwater-sampling site is located in a flat depression of a typical peak-cluster depression area (24.73N, 108.32E) (Fig. 1). This area experienced severe deforestation over nearly 30 years from 1958 to the mid-1980s and has been under natural restoration for almost 25 years. Currently, the vegetation can be classified into three secondary communities: tussock, shrub, and secondary forest. Almost 70% of the hillslopes are dominated by tussocks and shrubs. Most of the trees are found on dolo-

mite outcrops and nearby soils, or in the deep soils (>100 cm) at the foot of hillslopes. The calcareous soils are developed from dolomite and contain significant amounts of rock fragments, with a natural pH value between 7.1 and 8.0. Rainwater samples were collected using an automatic precipitation sampler (APS-2B, Changsha Xianglan Scientific Instruments Co., China), which automatically collects a rainwater sample for every rainfall event. The sampler consists of a rain collector, rain sensor, rain container and a dust-prevention hood. When a rain event occurs, the dust-prevention hood opens within 60 s, and closes 5 min after the rainfall stops. The sampler was placed approximately 120 cm above the ground. In addition, individual sampling was performed at 9:00 am on a daily basis, following a precipitation event. Rainwater samples were immediately transferred to the laboratory for analysis of electrical conductivity (EC) and pH. They were then filtered through 0.45 μm pore size membrane filters to remove insoluble particles, and stored in a refrigerator at around 3–5°C prior to chemical analysis. Concentrations of Cl^-, NO_3^-, SO_4^{2-}, K^+, Na^+, Ca^{2+}, Mg^{2+}, and NH_4^+ in 42 samples were sampled and analyzed during the monitoring period (June, 2007 to March, 2008). In addition, seven extra samples were collected with a large polyethylene sheet in order to determine the S isotope composition of sulfate ($\delta^{34}S–SO_4^{2-}$). The amount of rainfall was determined by automatic equipment in the meteorological zone of the study site. A pH meter with a combination glass electrode was used for pH measurement. The pH meter was calibrated before each measurement by using standard buffer solutions at pH 4.00 and 6.86. The EC measurement was made by using a digital conductivity meter with temperature compensation, which was periodically calibrated against KCl standard solutions. The anions of Cl^-, NO_3^-, and SO_4^{2-} were measured by ion chromatography (Dionex DX-120) with a precision of 5%. The cations of K^+, Na^+, Ca^{2+}, Mg^{2+} were measured with an Inductively Coupled Plasma Optical Emission Spectrometer (ICP-OES Varian Vista MPX) with a precision better than 5%. NH_4^+ was determined spectrophotometrically using the Nessler's reagent colorimetric method. Reagent and procedural blanks were determined in parallel with the sample treatments, using identical procedures. Each calibration curve was evaluated against analyses of these quality control (QC) standards before, during, and after the analyses of a set of samples. Sulfate was recovered from precipitates of $BaSO_4$ with enough 2 mol/L $BaCl_2$ solution to determine the $\delta^{34}S–SO_4^{2-}$. After precipitating for 15 min, the mixture was filtered through 0.22 μm acetate membrane filters. The precipitates ($BaSO_4$) on the filters were carefully rinsed with sufficient Milli-Q water to remove Cl^-. The precipitates were then immediately transferred into crucibles with the filters and combusted at 800°C for 40 min in air. Then, the $BaSO_4$ in the crucible was crushed to a fine powder. Finally, 0.5 mg of the $BaSO_4$ powder of each sample was weighed and wrapped in a tin cup, and analyzed using an IsoPrime continuous flow mass spectrometer. The analytical results are expressed in the usual δ, in per mil, relative to Canyon Diablo Troilite (CDT) standard. The standard deviation of the isotopic measurements is 0.2‰ (n = 10).

Table 1. Mean concentration (in μeq/L) of major ionic components, pH (in unit) and EC (in μS/cm) in rainwaters, along with statistical results parameters

	VWV	Mean	Median	SD	Min	Max
pH	5.1	5.2	5.3	0.5	4.2	6.2
EC	24.5	35.2	29.5	20.3	8.0	97.0
NH_4^+	56.6	86.3	59.4	81.5	3.0	396.2
Na^+	15.4	15.3	14.9	9.2	1.7	42.2
K^+	7.2	7.4	6.0	4.2	0.7	16.8
Ca^{2+}	70.7	102.5	102.6	53.7	21.9	219.6
Mg^{2+}	34.4	56.1	51.3	42.1	0.2	190.2
Cl^-	18.1	18.6	16.8	10.3	5.5	44.1
SO_4^{2-}	118.4	181.0	132.8	127.7	36.4	585.6
NO_3^-	8.5	12.8	8.4	9.8	1.3	35.0
$TZ^- – TZ^+$	–39.4	–55.3	–76.2			

VWM, volume-weighted mean; SD, standard deviation; Min, minimum; Max, maximum.
$TZ^- – TZ^+$, sum of anions – sum of cations.

Results and Discussion

The calculated volume-weighted means (VWM) and standard deviations for the concentrations of the main chemical components are summarized in Table 1. The ion concentration data generally exhibited a high relative standard deviation, indicating a large variability in the cation and anion concentrations between the rain events.

pH and EC

The pH values of individual precipitation collections ranged from 4.2 to 6.2, with a VWM of 5.1 (Table 1). Around 12% of the rainwater samples had pH < 4.5, and 76.2% of the total precipitation had pH < 5.6. Typically, the dissolution of naturally occurring CO_2, NO_x, and SO_2 into clouds and droplets results in rain in the clean atmosphere with pH values of between 5.0 and 5.6 (Charlson and Rodhe, 1982). Rainwater with a pH value below five is caused by the presence of natural H_2SO_4, weak organic acids, or anthropogenic emission of H_2SO_4 and/or HNO_3. Samples with pH values above 6.0 may be the result of dissolution of windblown dust with a high $CaCO_3$ content, derived from the weathering of carbonate. Under such conditions, the high pH value does not correspond to a high HCO_3^- concentration. Even at pH >

Table 2. Comparison of the major ion concentrations (μeq/L) and pH values in Huanjiang with other sites worldwide

Site	pH	Cl^-	NO_3^-	SO_4^{2-}	NH_4^+	K^+	Na^+	Ca^{2+}	Mg^{2+}	SO_4^{2-}/NO_3^-	TZ	Rainwater type	References
Huanjiang	5.1	18.1	8.5	118.4	56.6	7.2	15.4	70.7	34.4	12.6	282.3	Rural	This study
Chengdu	4.4	42.3	30.4	331.6	250.7	20.8	22.6	192.0	13.2	10.9	903.6	City	Lei *et al.* (1997)
Chongqing	4.6	40.3	43.2	221.8	386.6	15.2	69.8	207.2	13.2	5.1	997.3	City	Lei *et al.* (1997)
Guiyang	4.5	21.2	48.2	188.0	—	11.0	4.0	113.2	25.5	3.9	411.1	City	Han *et al.* (2010)
Lanzhou	7.7	27.9	74.4	208.0	57.2	7.3	12.3	88.6	46.5	2.8	522.2	City	Xu *et al.* (2009)
Massif (France)	5.2	19.6	36.2	22.3	—	5.7	14.4	14.6	3.4	0.6	116.2	Marine	Négrel and Roy (1998)
Adirondack (USA)	4.5	2.1	22.6	36.9	10.5	0.3	1.6	3.59	1.0	1.6	78.7	Megacity	Ito *et al.* (2002)
Tokyo (Japan)	4.5	55.2	30.5	50.2	40.4	2.9	37.0	24.9	11.5	1.6	252.6	Megacity	Okuda *et al.* (2005)
Beijing	5.1	104.0	109.0	315.8	185.6	17.7	25.0	607.2	40.4	2.9	1404.7	Megacity	Xu and Han (2009)
Leigongshan	4.4	1.1	26.0	75.0	33.0	4.1	2.9	25.0	5.1	2.9	172.2	Remote	IMPACTS (2004)
Maolan	5.1	9.5	2.9	39.2	56.8	6.9	6	14.8	2.6	13.5	138.7	Remote	Han *et al.* (2010)
Caijiatang	4.3	5.4	55.0	155.0	108.0	8.1	5.9	35.0	8.9	2.8	381.3	Rural	IMPACTS (2004)
Linan	4.4	8.1	38.7	86.7	6.8	8.5	52.4	57.2	29.2	2.2	287.6	Rural	Li *et al.* (2010)
Liuxihe	4.6	5.6	26.0	88.0	26.0	9.0	33.0	59.0	16.0	3.4	262.6	Rural	IMPACTS (2004)
Longfengshan	4.6	5.5	40.3	99.9	6.7	5.6	130.8	14.7	4.1	2.5	307.4	Rural	Li *et al.* (2010)
Puding	5.7	13.9	17.0	152.4	33.1	9.1	10.8	155.8	3.9	9.0	396.0	Rural	Wu *et al.* (2012)
Shangdianzi	4.3	23.7	102.9	257.6	17.0	12.5	393.0	120.2	37.1	2.5	964.0	Rural	Li *et al.* (2010)
Tieshanping	4.1	4.5	35.0	184.0	76.0	8.4	2.9	58.0	8.9	5.3	377.7	Rural	IMPACTS (2004)
Liuconguan	4.9	8.3	18.0	255.0	51.0	18.0	7.7	155.0	38.0	14.2	551.0	Sub-urban	IMPACTS (2004)

TZ, Sum of all ions.

5.6, the concentration of HCO_3^- in our samples was below detection. Although the study site is located in the central part of the Chongqing–Guiyang–Liuzhou acid rain control zone (Hao *et al.*, 2001), the pH values observed here were higher than those observed at other sites in this same zone, including Guiyang (Han and Liu, 2006) and Chongqing (Lei *et al.*, 1997), and were the same as was seen in neighboring Maolan (Han *et al.*, 2010, but lower than that of Puding (Wu *et al.*, 2012), which is a rural site mainly covered by farmland.

The EC values of rainwater samples range from 8.0 to 97.0 μS/cm, with a volume-weighted mean of 24.5 μS/cm (Table 1). This is around 10.0 μS/cm higher than that measured at Waliguan (Tang *et al.*, 2000), which represents the background value of the northern Tibetan Plateau, but lower than that of Shangdianzi, Linan, and Longfengshan (Li *et al.*, 2010), which are the regional background stations of north China, southeast China and northeast China, respectively. It is much lower than that of Beijing (Xu and Han, 2009), which is a metropolis. The EC of rainwater is mainly controlled by the total soluble ionic components, and the low EC values here reflect good environmental quality of the atmosphere in the study area. They may also indicate a preferable dilution effect to the atmospheric pollution, because of the abundant rainfall prevalent in the south, relative to the north of China.

Soluble ionic compositions of wet precipitation

Most of the rainwater samples had total cation concentrations ($TZ^+ = K^+ + Na^+ + Ca^{2+} + Mg^{2+} + NH_4^+$) larger than the total anion concentrations ($TZ^- = SO_4^{2-} + NO_3^- + Cl^-$), and the anion deficit ($TZ^- - TZ^+$) ranged from 41.0 to –181.5 μeq/L, with a mean of –55.3 μeq/L (Table 2). This imbalance is usually attributed to unmeasured organic anionic species, such as acetate, formate, $HCOO^-$, and CH_3COO^-, amongst others. For example, studies showed that organic acids were estimated to account for 8.1% in Anshun (Zhang *et al.*, 2011), which means that organic ionic species may account for a certain proportion of the total anionic deficit in the precipitation in southwest China.

It is clear that the Huanjiang rainwater has more Ca^{2+}, NH_4^+, Mg^{2+}, and SO_4^{2-}, compared with K^+, Na^+, Cl^-, and NO_3^- (Table 1). The mean concentration of ionic species in precipitation decreased in the following order: $SO_4^{2-} > Ca^{2+} > NH_4^+ > Mg^{2+} > Cl^- > Na^+ > NO_3^- > K^+$. Among these ions, SO_4^{2-}, Ca^{2+}, NH_4^+, and Mg^{2+} were the dominant ions, generally accounting for more than 80% of the total ionic concentration. These results are similar to the results from previous studies in southwest China (Aas *et al.*, 2007; Han and Liu, 2006; Han *et al.*, 2010; Lei *et al.*, 1997; Wu *et al.*, 2012). Ca^{2+} was the most abundant cation, with a concentration ranging from 21.9 to 219.6 μeq/L, with a mean of 102.5 μeq/L. NH_4^+ was the second most abundant cation in the rainwater samples, with concentrations varying from 3.0 to 396.2 μeq/L, with a mean of 86.3 μeq/L. Ca^{2+} and NH_4^+ together accounted for 44–84% of the total cations measured, with a mean of 70%. SO_4^{2-} was the dominant anion; its concentration ranged from 36.4 to 585.6 μeq/L, with a mean of 181.0 μeq/L, accounting for 61–94% of the total anions measured, with a mean of 82.5%. Cl^- and NO_3^- both had concentrations ranging from 5.5 to 44.1 μeq/L and 1.3–35.0 μeq/L, with means of 18.6 and 12.8 μeq/L, respectively.

A comparison of the major ion concentrations and pH values in Huanjiang with other sites worldwide is given in Table 2. Generally, the total ion concentrations (TZ) increased in the order of remote site < rural site < city

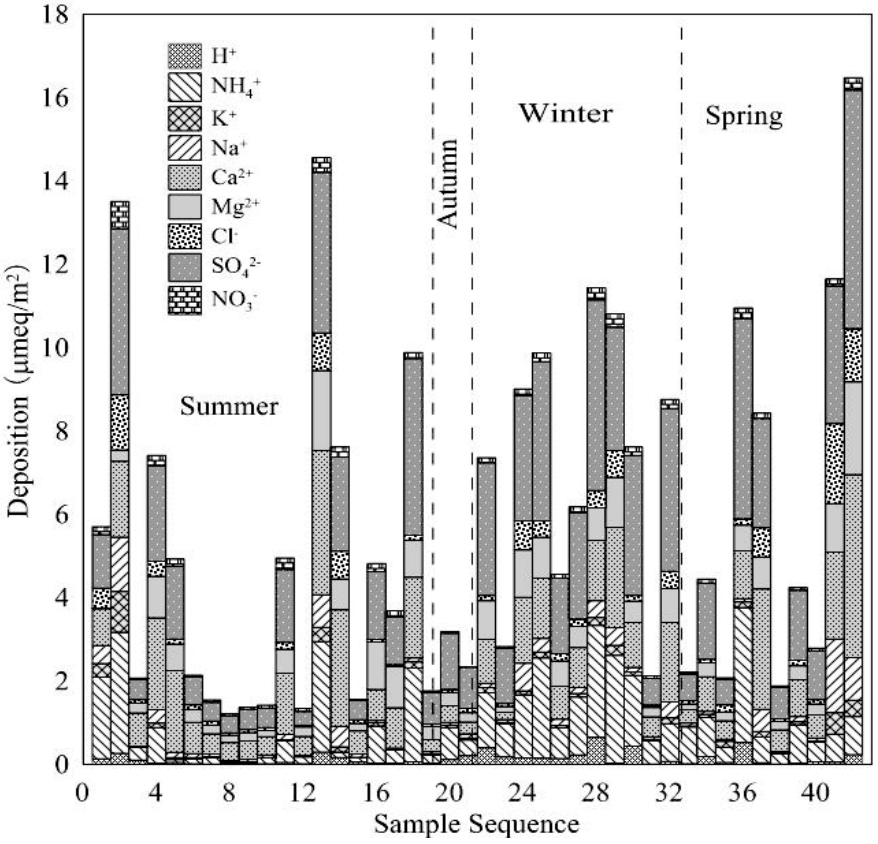

Fig. 2. Daily wet deposition fluxes of ionic components.

site < megacity site (Table 2). However, Shangdianzi had higher TZ than that of Lanzhou (Xu *et al*., 2009) and Chengdu (Lei *et al*., 1997). This may be because Shangdianzi is situated in Miyun County within the Beijing Municipality, and surrounds the core of Beijing–Tianjin–Hebei, where huge populations and industries are concentrated (Aas *et al*., 2007; Li *et al*., 2010). The TZ of our study area was significantly higher than TZs observed in Leigongshan (IMPACTS, 2004) and Maolan (Han *et al*., 2010), which are both covered with thick forest, and represent the background value for southwest China, but are much lower than those in cities and megacities such as Beijing (Xu and Han, 2009), Shanghai (Huang *et al*., 2008), Chengdu and Chongqing (Lei *et al*., 1997). Huanjiang had a lower TZ compared to Shandianzi, Longfengshan, and Linan, which are the regional background stations for the north, southeast, and economically developed Yangtze River Delta of China, respectively (Li *et al*., 2010). The SO_4^{2-} concentration was higher than that observed in Maolan and Leigongshan, but lower than that of other rural sites and cities. However, NO_3^- in this study was very low, only slightly higher than that of the Maolan remote site, and much lower than other rural and city sites. The NH_4^+ concentration was the same as that of Maolan, but much lower than that observed in large cities. The concentration of Ca^{2+} was higher than that observed in the regional background sites Maolan, Leigongshan, and Longfengshan, but lower than that of cities. Further, we compared our results with worldwide monitored data, revealing that the ionic concentrations (such as SO_4^{2-}) of the precipitation in our study area were higher than that of reference cities in Europe (Négrel and Roy, 1998), North America (Ito *et al*., 2002), and Southeast Asia (Okuda *et al*., 2005). However, the NO_3^- concentration was much lower, compared to these cities. In addition, the SO_4^{2-}/NO_3^- ratio was much higher than that seen in all cities listed in Table 2.

Ionic wet deposition fluxes

The changes in the daily ionic deposition fluxes were calculated by multiplying the ionic concentrations from individual precipitation events by the rainfall amount; values are illustrated in Fig. 2. The daily ionic deposition fluxes showed large variations, with the highest flux occurring in spring. The amount of rainfall from June 2007 to May 2008 was 1333.6 mm, of which 455.2 mm fell in spring (March–May), 669.0 mm in summer (June–August), 101.8 mm in autumn (September–November),

Table 3. Correlation coefficients (R) of ionic concentrations in rainwater samples of Huanjiang. Bold values indicate a significant correlation

	NH_4^+	K^+	Na^+	Ca^{2+}	Mg^{2+}	Cl^-	SO_4^{2-}	NO_3^-
NH_4^+	1							
K^+	**0.661**	1						
Na^+	0.180	0.279	1					
Ca^{2+}	0.303	0.113	0.362	1				
Mg^{2+}	0.379	0.313	0.226	**0.711**	1			
Cl^-	0.228	0.370	**0.950**	0.436	0.256	1		
SO_4^{2-}	**0.869**	**0.572**	0.277	**0.587**	**0.605**	0.323	1	
NO_3^-	**0.557**	0.348	0.236	**0.784**	**0.721**	0.302	**0.706**	1

and 107.6 mm in winter (December–February). Annual and seasonal variations in the deposition fluxes were calculated. The results showed that, among the ions, SO_4^{2-} had the maximum deposition flux, with a mean of 157.9 meq/m^2, followed by Ca^{2+} with a mean of 94.2 meq/m^2, NH_4^+ with a mean of 75.5 meq/m^2, Mg^{2+} with a mean of 45.9 meq/m^2, and Na^+ with a mean of 20.5 meq/m^2. The deposition loading of the above-mentioned major ions accounts for almost 88.4% of the total wet deposition.

Seasonal differences in wet deposition fluxes are apparent in all of the ionic components. Although the VWMs of TZ were ordered by autumn > winter > spring > summer, the highest wet deposition of most of the ions was observed in the summer, due to the higher rainfall and higher frequency of rain events, with the exception that SO_4^{2-} and NH_4^+ had their highest fluxes in spring. Wet deposition fluxes of major ionic species in winter were lowest because of the relatively lower rainfall at this time. In general, precipitation in southwestern China is high in the spring and summer, and low in the autumn and winter. Thus, a significant correlation between the amount of rainfall and the seasonal variation in wet deposition fluxes is revealed.

Origins of major ionic species

Statistical analysis In order to find the associations between ions in the precipitation, as well as the possible sources of pollutants, we determined the correlations between ions in the precipitation and we have depicted these in Table 3. Good correlations were observed between sulfate and nitrate, which may be attributable to the similarities in their chemical behaviors in precipitation, and the co-emission of their precursors SO_2 and NO_x. There was a good correlation between Ca^{2+} and Mg^{2+} (R = 0.711), which is to be expected because of their chemical similarity. This is consistent with the wide distribution of carbonate in the sampling site; the result is the same as those in other karst dominated areas (Han and Liu, 2006; Han *et al.*, 2010; Wu *et al.*, 2012). Similarly, significant correlations were also observed between the sea-salt species Na^+ and Cl^-, indicating a common marine source. SO_4^{2-} shows good corrections with NH_4^+, K^+ Ca^{2+}, and Mg^{2+}, with correlation coefficients of 0.869, 0.572, 0.587, and 0.605, respectively. Moreover, NO_3^- also showed good corrections with NH_4^+, Mg^{2+}, and Ca^{2+}, with coefficients of 0.557, 0.721, and 0.784, respectively. These observed correlations in the local precipitation are thought to be caused by atmospheric chemical reactions of the acids H_2SO_4, HNO_3, and HCl with alkaline compounds abundant in carbonate materials, which have been carried into the atmosphere as wind-blown particulate matter. Ca^{2+} and Mg^{2+} are major components of the earth's crust, while NH_4^+ mainly originates from anthropogenic activities such as agricultural activity and biomass burning. The association of SO_4^{2-} with Ca^{2+}, Mg^{2+} and NH_4^+, as well as NO_3^- with NH_4^+, Ca^{2+}, and Mg^{2+}, may be attributable to atmospheric chemical reactions with one another, indicating that NH_4^+, Ca^{2+} and Mg^{2+} play a major role in neutralizing acidic sulfur and nitrogen gas. The predominant species combinations were NaCl, $CaSO_4$, $MgSO_4$, $(NH_4)_2SO_4$, K_2SO_4, NH_4NO_3, $Ca(NO_3)_2$, and $Mg(NO_3)_2$, which may accumulate within atmospheric water droplets by aerosol scavenging and also by subsequent reaction of gaseous species on the aerosol. The correlation of NH_4^+ to SO_4^{2-} (R = 0.869) was higher than that of NH_4^+ to NO_3^- (R = 0.557), showing that sulfur compounds are likely dominant in the atmosphere; this is same as was found in previous studies (Wu *et al.*, 2012).

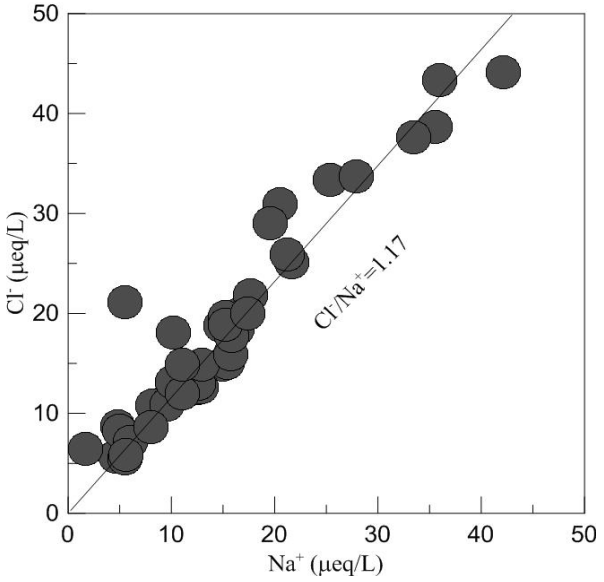

Fig. 3. Relationship between Na^+ and Cl^- in the rainwater samples. The line in the diagram shows the corresponding ratios of seawater.

Enrichment factors and source contributions Element

Table 4. Enrichment factors for rainwater components relative to soil and seawater

		Na^+	K^+	Ca^{2+}	Mg^{2+}	Cl^-	SO_4^{2-}	NO_3^-
	$[X/Na^+]_{sea}$	—	0.0218	0.0439	0.227	1.16	0.125	—
	$[X/Na^+]_{rain}$	—	0.472	4.600	2.242	1.176	7.700	—
EF_{sea}		—	21.64	104.79	9.88	1.01	61.60	—
	$[X/Ca^{2+}]_{soil}$	0.569	0.504	—	0.561	0.0031	0.0188	0.0021
	$[X/Ca^{2+}]_{rain}$	0.217	0.103	—	0.487	0.256	1.676	0.120
EF_{soil}		0.38	0.20	—	0.87	82.45	89.15	57.14

Crustal S and N are regarded as entire SO_4^{2-} and NO_3^- compounds, respectively (from Taylor, 1964).

enrichment factors (EFs) are widely used in environmental sciences to speculate on the origin of elements in air, atmospheric dust or precipitation (Reimann and Caritat, 2000). Their calculation is based on the elemental ratio found between ions collected in the atmosphere and in precipitation, compared to a similar ratio in a reference material. EF values may impart information about the source of the element. Commonly, Na is taken as the best reference element for seawater since it is assumed to be of purely marine origin. Al and Ca are two typical lithospheric elements and are normally used as reference elements for continental crust, since their compositions in soil, the only natural source for lithospheric elements, rarely change. Compared with seawater, the rainwaters collected in this study mostly had Cl^-/Na^+ equivalent ratios greater than that (Cl/Na = 1.17) of seawater (Fig. 3). In order to estimate the marine and terrestrial contributions to rainwater, the EF values for rainwater compositions were calculated, using Na as a reference element for marine origin and Ca as a reference element for continental origin, as follows:

$$EF_{seawater} = [X/Na^+]_{rainwater}/[X/Na^+]_{seawater}$$

$$EF_{soil} = [X/Ca^{2+}]_{rainwater}/[X/Ca^{2+}]_{soil}$$

where X is the concentration of the ion of interest, $X/Na^+_{seawater}$ is the ratio within seawater (Keene *et al.*, 1986) and X/Ca^{2+}_{soil} is the ratio within the crust (Taylor, 1964). All concentrations used in the calculation of EF for sea salt components and soil components are expressed in the same units, μeq/L and ppm, respectively. The contribution of NO_3 and NH_4 from marine sources is negligible, therefore EFs for a marine source were computed for Cl, Mg, K, and SO_4, and EFs for a soil source were computed for K, Mg, Cl, SO_4, and NO_3. Table 4 gives the EF values for soil and sea salt components. An EF value much higher than 1 is considered to be other source rather than reference source. Cl^- has $EF_{seawater}$ value of 1.01, but has an EF_{soil} value of 82.45. This clearly points toward a marine origin for Cl^-. Mg^{2+} and K^+ seemed to be diluted by seawater and concentrated by soils. Mg^{2+} was partly derived from a marine source, but the contribution from soil is also considerable. Average $EF_{seawater}$ values of K^+ and Ca^{2+} were 21.64 and 104.79, respectively, suggesting that most of the K^+ and Ca^{2+} originate from terrestrial sources. SO_4^{2-} was largely enriched relative to the soil (EF = 89.15) and a marine source (EF = 61.6). These high EF values indicate that the contribution of SO_4^{2-} from both soil and marine sources was almost negligible, so SO_4^{2-} is mainly derived from anthropogenic sources. Generally, the marine source of NO_3^- was quite small. Therefore, anthropogenic activities were also considered to be the major source of nitrate.

In order to estimate the marine and crustal contributions to different ionic species in rainwater, their respective sea salt fraction (SSF) and crust fraction (CF) were calculated, using the following equations:

$$\%SSF = 100(X/^+Na)_{seawater}/(X/^+Na)_{rainwater}$$

$$\%CF = 100(X/Ca^{2+})_{soil}/(X/Ca^{2+})_{rainwater}.$$

Figure 4 and Table 5 show the fractions of these sources for an individual precipitation event and their VWM values, respectively. Although the fractions were different in each precipitation event, the calculations revealed that nearly all the Cl^- (98.6%) was of marine origin. In addition, only small amounts of rainwater seemed to have a significant anthropogenic fraction (AF) of Cl^- (Fig. 4), which could be derived from agricultural activities in the rural background (Han *et al.*, 2010). In contrast, SO_4^{2-}, Ca^{2+}, K^+, and Mg^{2+} appear to be of non-marine origin. As mentioned previously, the bedrock of the study site is dolomite, which weathers to produce a soil that is rich in Ca and Mg. The study site was located in the flat depression of a typical karst peak-cluster depression; soil and sand can be produced from the peak cluster surrounding it, which facilitates the generation of alkaline dust particles by the wind. We therefore conclude that the Ca^{2+} and Mg^{2+} most likely originates from crustal sources, either from dolomite weathering or from long-range transport from large cities in the surrounding area. The origin of K^+ must be different to that of Ca^{2+} and Mg^{2+}, due to the

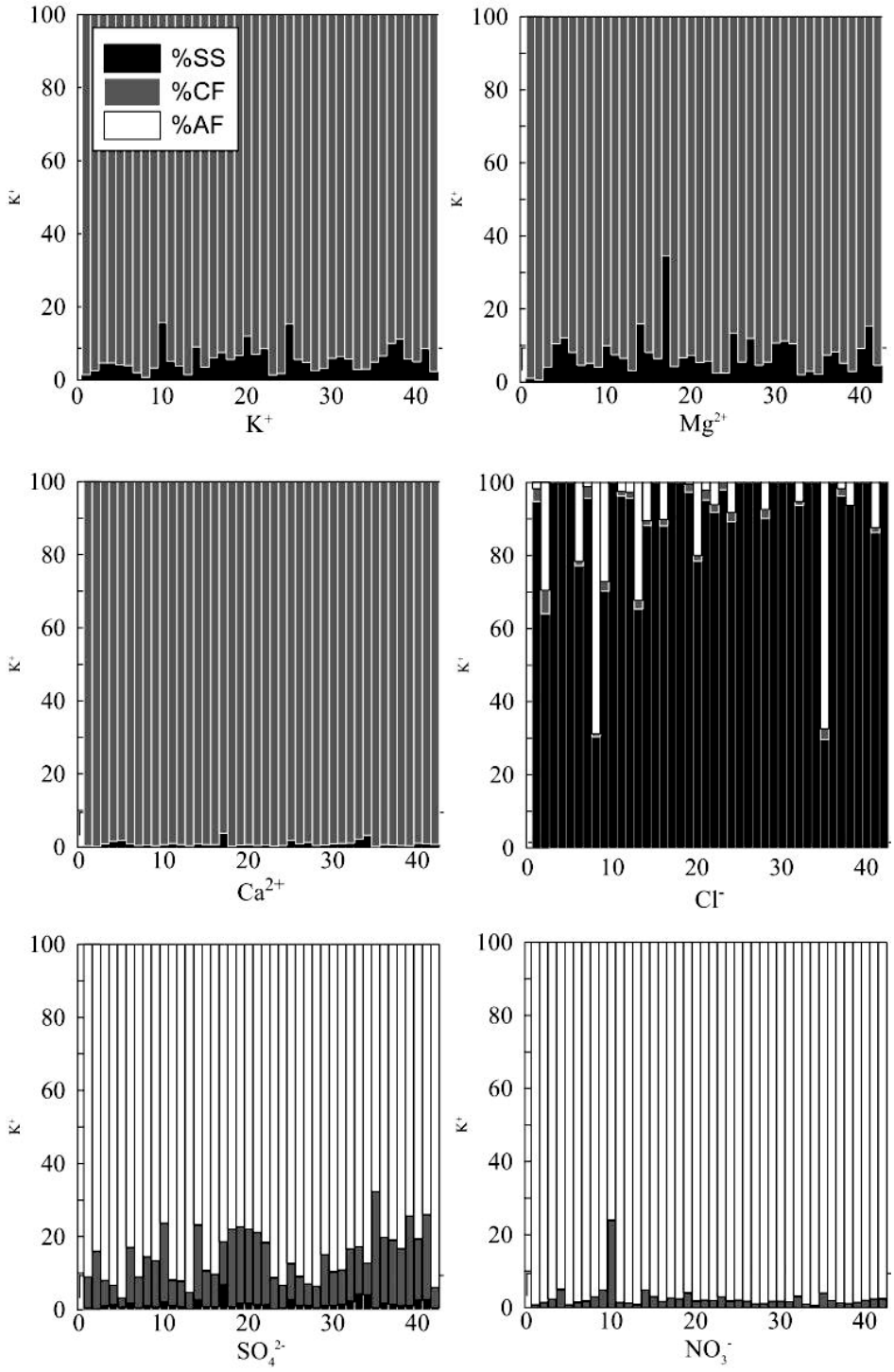

Fig. 4. Sea salt fraction (%SSF), crust fraction (%CF), and anthropogenic fraction (%AF) of ionic species in an individual precipitation event. The x-axis represents the sample sequence.

poor correlation of K^+ with them. K^+ in the atmosphere is generally considered as a chemical signature of biomass burning (Dibb *et al.*, 1996). It occurs usually in coarse particles in soil, but fine particles can be created by wood combustion. In fact, wood combustion is common in residential cooking and other agricultural activities. In this data, the primary source of K^+ is considered to be terrestrial, because it is difficult to quantitatively distinguish

Table 5. Source contributions for different ionic constituents in rainwater

Ions	Sea salt fraction (%)	Terrestrial fraction (%)	
		Crust fraction	Anthropogenic source fraction
SO_4^{2-}	4.6	1.12	94.3
NO_3^-	—	1.75	98.3
Cl^-	98.6	1.2	0.2
K^+	4.6	95.4	
Ca^{2+}	1.0	99.0	
Mg^{2+}	10.1	89.9	

the soil source from wood combustion in the precipitation samples.

Unlike Ca^{2+} and Mg^+, SO_4^{2-} had a tiny contribution from the crustal source; about 94.3% of the total SO_4^{2-} was derived from anthropogenic sources (Table 5). Coal combustion accounts for approximately 70% of commercial energy production in China, leading to substantial SO_2 emissions, which to date have been the most important precursor for acid rain in China (Aas *et al*., 2007). This is further corroborated by $\delta^{34}S$–SO_4^{2-} results (see Subsubsection "$\delta^{34}S$–SO_4^{2-} constrains on anthropogenic SO_4^{2-}" for details).

Assuming no nitrate is derived from the marine source, the contributions from anthropogenic sources were obtained by subtracting the soil contribution from the total nitrate in rainwater. From this, around 98.3% of NO_3^- was attributed to anthropogenic sources (Table 5). NO_3^- in rainwater results from both human activities such as fuel combustion, and chemical reactions in the atmosphere. NO_3^- concentrations at this site were lower than in other rural and urban areas (Table 3), because the study site is far away from intense human activities and urban emissions, such as those from traffic and cement works, as they are largely absent in this rural study area.

As discussed previously, NH_4^+ was the second most dominant cause of acid neutralization in the sampled rainwater, with a VWM of 56.6 μeq/L, which is similar to that found at Maolan (Han *et al*., 2010), and was consistent with a previous study that found ammonia emissions in the Asian region to be typically several times higher than those in North America and Europe (Galloway, 1995). Livestock feeding, nitrogen-rich fertilizer and soil are regarded as the main emission sources of NH_4^+. Although the study site has been under natural restoration for almost 25 years, livestock feeding is common in local areas, and there are large areas of farmland surrounding the study site. The good correlation of NH_4^+ with K^+ (Table 3) may indicate their co-emission. Therefore, livestock feeding, agricultural activities and biomass burning are inferred to be the source of the NH_4^+ detected in the rainwater. Forest soils may also make a large contribution, because NH_3 volatilization from soil increases as the soil pH increases; pH values of soil in the study site are around 7.1–8.1, which suggests the potential emission of NH_3.

Anthropogenic sources Results of EFs analysis showed that SO_4^{2-} and NO_3^- mainly had an anthropogenic origin. We further analyzed the relationship between anthropogenic SO_4^{2-} ($SO_4^{2-}{}_{AF}$) and NO_3^- ($NO_3^-{}_{AF}$) using the EF-based results, they are shown in Fig. 5.

As discussed above, good correlations between sulfate and nitrate (Table 3) may be attributable to the similarities in their chemical behaviors and the co-emission of their precursors SO_2 and NO_x. If the precursors were the same for all of the precipitation events, there should be a better relationship between $SO_4^{2-}{}_{AF}$ and $NO_3^-{}_{AF}$. However, the observations were different to this (Fig. 5), which may be due to the influences of air masses, including their origin and passes. Therefore, precipitation events were categorized based on air-mass back-trajectories generated using Hybrid-Single Particle Integrated Trajectories (HYSPLIT 4), provided by the National Oceanic and Atmospheric Administration (NOAA) Air Resource Laboratory (Rolph, 2011). For each precipitation event, a 24 h backward trajectory was initiated at the recorded onset of precipitation, from 1000 m above ground level over the sampling site. On the basis of these trajectories, the precipitation events were divided into four types (Fig. 6): Southwest Asia and China (Type SW), South China and Asia (Type S), Northeast China (Type NE), and Southeast China (Type SE). The relationships between $SO_4^{2-}{}_{AF}$ and $NO_3^-{}_{AF}$ of these four event types are shown in Fig. 7.

$SO_4^{2-}{}_{AF}$ and $NO_3^-{}_{AF}$ in samples from precipitation events of each type show good linear relationships, with a few exceptions of samples with low rainfall amounts (Fig. 7). This indicates the co-emission of the ions' precursors SO_2 and NO_x. However, precipitation events of type SW (Fig. 7a), type S (Fig. 7b), and type NE (Fig. 7c) show better linear relationships than that of type SE (Fig. 7d). Abnormal precipitations of type SW (Fig. 7a) and NE (Fig. 7c), which generally occurred during the dry season, all show higher $(SO_4^{2-}/NO_3^-)_{AF}$ ratios than the mean. In contrast, those of type SE, which mainly occurred during the growing/wet season, had lower ratios than the mean (Fig. 7d). The abnormal $(SO_4^{2-}/NO_3^-)_{AF}$ ratios in precipitation events of type SW and type NE may be due to the negative correlation of atmospheric SO_2 concentration with rainfall amount (Pena *et al*., 1982), meaning that small amounts of precipitation can dissolve more SO_2 from the atmosphere. However, this cannot be the reason for abnormal $(SO_4^{2-}/NO_3^-)_{AF}$ ratios in type SE precipitation. The rainwater that was collected in time-sequence in the continuous precipitation of June, 12, 2008, which was of type SE, showed large variations in SO_4^{2-}/

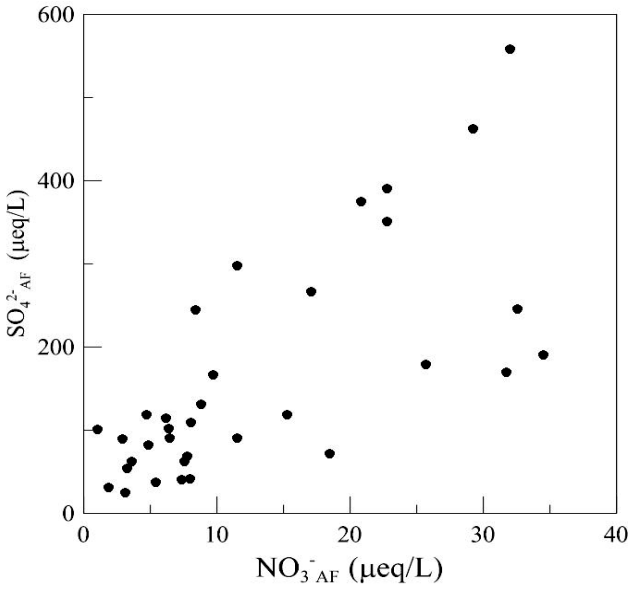

Fig. 5. Relationship between anthropogenic SO_4^{2-} ($SO_4^{2-}{}_{AF}$) and NO_3^- ($NO_3^-{}_{AF}$) in rainwaters.

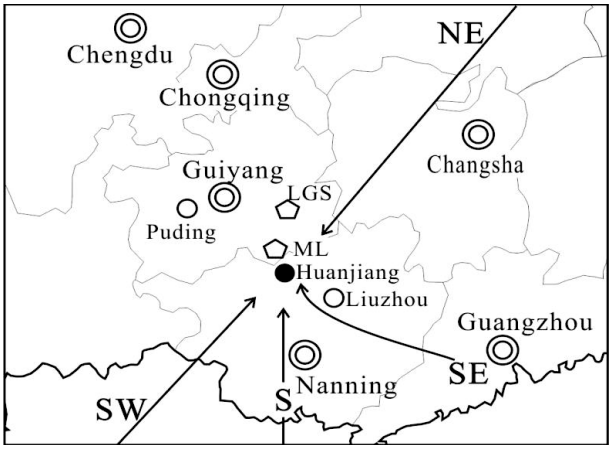

Fig. 6. Four air mass backward trajectory types generated at the 1000 m level. SW, S, SE, and NE represent clusters of Southwest Asia and China, Southeast China, Northeast China, and South China and Asia, respectively.

NO_3^- ratios, ranging from 7.5 to 47.3 (n = 12), and were not associated with the quantity of precipitation (unlisted in table), which perhaps implies the involvement of variable sources or processes in altering the SO_4^{2-} and/or NO_3^- concentrations of the precipitation. High concentrations may be attributable to the industrial plume from the upwind urban area (Fig. 6). In addition, significant urban and industrial emissions are noted for Liuzhou city, which is one of the most important heavy industrial cities of China, renowned for its automotive, metallurgical, and mechanical industry.

The VWMs of pH and ion concentrations based on air mass back-trajectories are shown in Table 6. The concentrations of TZ from the marine storms (S and SW) were lower than those from the continental storms (NE and SE). For the majority of these ions, the highest concentrations were observed in rain events of type SE, which are mostly predominant in the winter/dry season. The lowest concentrations of TZ were found in type SW and S events, when air masses travel from marine storms during the Southern Asian Monsoon period with very high rainfall volumes.

As described above, the VWM of the SO_4^{2-}/NO_3^- ratio (Table 2) in the study area was lower than that of the cities listed in Table 2, and was almost equal to that of rural/remote sites like Puding (Wu *et al*., 2012) and Maolan (Han *et al*., 2010), suggesting that the contributions of traffic emissions to atmospheric pollution in the study area were insignificant. Precipitation from the SW had the lowest SO_4^{2-}/NO_3^- ratio (8.9) among the four types of precipitation; this could be due to the traffic emissions of Hechi City situated 25 km away from the study site (Fig. 6). This is further supported by the range of lower SO_4^{2-}/NO_3^- ratios (3.2–5.4) in the rain of Hechi City in 2007–2008 (Qin *et al*., 2011).

$\delta^{34}S$–SO_4^{2-} constrains on anthropogenic SO_4^{2-} As discussed above, nearly 94.3% of SO_4^{2-} in the studied rainwaters was derived from anthropogenic sources. Here we use $\delta^{34}S$–SO_4^{2-} to further constrain these anthropogenic sources. The sulfate ion concentration of the non-sea salt (NSS) and its $\delta^{34}S$–$SO_4^{2-}{}_{NSS}$ was computed from the sodium ion concentration in the sample using methods described by Mizoguchi *et al*. (2012). The $\delta^{34}S$–$SO_4^{2-}{}_{sample}$ and $\delta^{34}S$–$SO_4^{2-}{}_{NSS}$ ranged from –5.6 to –11.0‰, and 11.4~–6.6‰, with average values of –8.4‰ and –9.1‰ (n = 7), respectively. The ratios were in the $\delta^{34}S$ range of local coal (–12.5~–2.1‰) (Xiao *et al*., 2010). Thus, we concluded that the SO_x produced by the combustion of local coal was the main source of anthropogenic sulfate in the rainwaters. This is same as was found in other studies of rain in China (Aas *et al*., 2007; Larssen *et al*., 2006; Mukai *et al*., 2001; Xiao and Liu, 2002). The $\delta^{34}S$–$SO_4^{2-}{}_{NSS}$ of precipitation of type SE, type SW, and type S were –10.7‰, –9.2‰, and –8.0‰, respectively, and we link these differences to different sulfate sources, as these samples were collected in the same season, between the end of May and the beginning of June, 2007. The differences in $\delta^{34}S$ caused by local biomass activities and other factors were negligible. In a study of $\delta^{34}S$ in atmospheric SO_2 in the south of China, negative values ranging –17.3~–13.6‰ were reported in Liuzhou city, which is located upwind of the SE direction precipitation events, around 190 km away from the

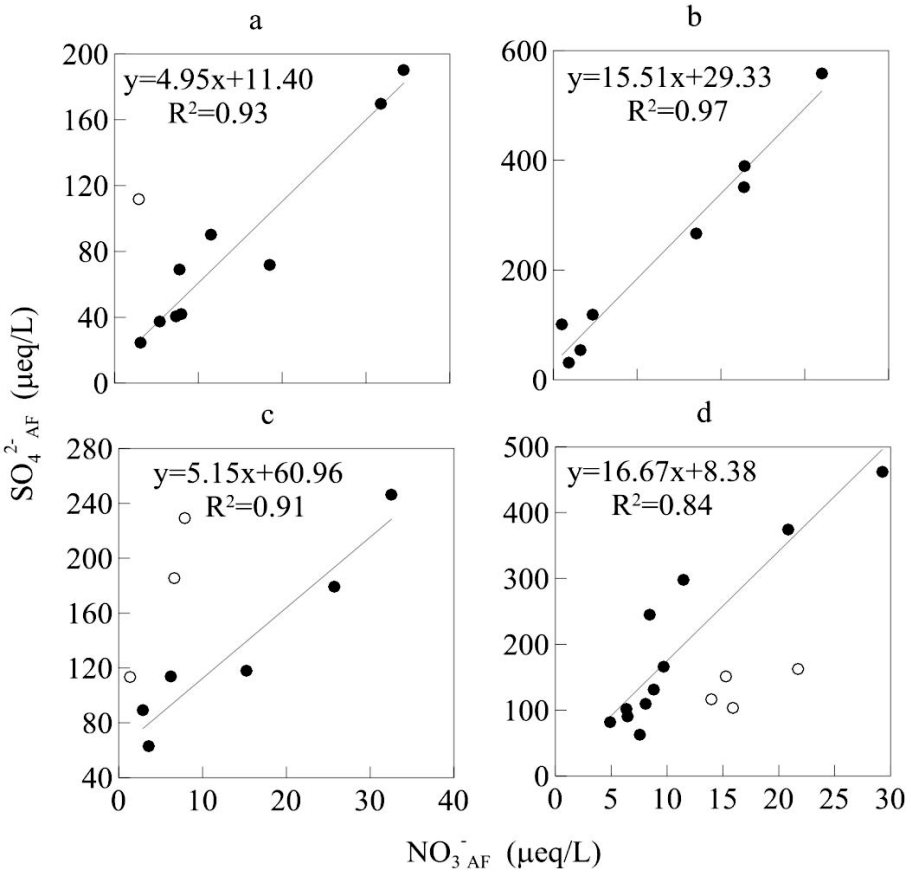

Fig. 7. Relationship between $SO_4^{2-}{}_{AF}$ and $NO_3^-{}_{AF}$ of precipitation, categorized by air mass back-trajectories. a, b, c, and d represent precipitation of type SW, S, NE, and SE, respectively. Hollow circles indicate precipitation events with a small amount of rainfall that were excluded from the calculation.

current study site (Zhang *et al*., 2002). Therefore, the lower $\delta^{34}S–SO_4^{2-}{}_{NSS}$ of type SE precipitation perhaps indicates that this negative SO_2 sulfate may contribute to the NSS sulfate of precipitation in this study. However, elucidating the precise fraction requires further study.

Impact of sulfate on carbon uptake by karst

Sulfuric acid contributes significantly to the chemical weathering of carbonate rocks in southwest China (Han and Liu, 2004; Li *et al*., 2008; Liu, 2007). However, studies that are mainly carried out in large rivers generally average the situation from various different backgrounds. Here we focused our study on the influence of sulfuric acid on carbonate weathering in a rural area.

Weathering and CO_2 consumption rate impacted by sulfuric acid The composition of the stream water draining through the studied site is mainly controlled by carbonate dissolution, however the sum of the concentrations of Ca^{2+} and Mg^{2+} ($[Ca^{2+}+Mg^{2+}]$) were in excess with respect to HCO_3^- ($[HCO_3^-]$), with a mean $[Ca^{2+}+Mg^{2+}]/[HCO_3^-]$ ratio of 1.1 (Ding, 2010). Sulfuric acid is thought to account for the excess of Mg^{2+} and Ca^{2+} relative to HCO_3^-, as NO_3^- and Cl^- together account for less than 5% of the total anions. Assuming that sulfuric and carbonic acid simultaneously attack carbonate minerals, the dissolution of carbonate can be described as follows:

$$Ca_{(2-x)}Mg_x(CO_3)_2 + 2H_2CO_3 = (2-x)Ca^{2+} + xMg^{2+} + 4HCO_3^-$$

$$Ca_{(2-x)}Mg_x(CO_3)_2 + H_2SO_4 = (2-x)Ca^{2+} + xMg^{2+}2HCO_3^- + SO_4^{2-}.$$

The average Mg^{2+}/Ca^{2+} ratio was 0.82 in the water, with a $[Ca^{2+}+Mg^{2+}]^*$ ($=[Ca^{2+}+Mg^{2+}–SO_4^{2-}]$) value of 5.5. Given the assumption that calcite dissolution and the SO_4^{2-} in the river water is balanced by Ca^{2+} and Mg^{2+}, we obtain an average molecular formula of $Ca_{1.1}Mg_{0.9}(CO_3)_2$, for the carbonate dissolved by the stream water. We can further obtain the dissolution reac-

Table 6. Volume-weight mean (μeq/L) of major ionic rain components and TZs based on air mass back-trajectories

Types (percent of rainfall, %)	pH	NH_4^+	K^+	Na^+	Ca^{2+}	Mg^{2+}	Cl^-	SO_4^{2-}	NO_3^-	S/N	TZ
NE (11.1%)	5.0	83.6	8.7	11.1	83.0	59.3	16.3	150.0	11.1	13.5	423.0
SE (22.2)	4.9	80.9	6.4	15.0	91.6	47.4	16.5	181.9	10.4	17.4	450.0
S (30.9)	5.3	44.1	5.0	14.0	47.2	21.6	16.4	91.6	4.7	19.4	244.6
SW (35.7)	5.3	40.3	7.8	14.1	57.1	21.1	16.1	70.1	8.5	8.2	235.1

tions of carbonate by only carbonic acid and by both sulfuric and carbonic acid, based on stoichiometry analysis, as follows, respectively:

$$Ca_{1.1}Mg_{0.9}(CO_3)_2 + 2H_2CO_3 = 1.1Ca^{2+} + 0.9Mg^{2+} + 4HCO_3^-$$

$$Ca_{1.1}Mg_{0.9}(CO_3)_2 + 1.5H_2CO_3 + 0.2H_2SO_4 = 1.1Ca^{2+} + 0.9Mg^{2+} + 3.5HCO_3^- + 0.2SO_4^{2-}.$$

Thus, the rate of carbonate weathering (TDS_{carb}) by only carbonic acid and by both sulfuric and carbonic acid can be calculated using the following equations, respectively:

$$TDS_{carb-H2CO3} = [Ca^{2+}]/1.1 + [Mg^{2+}]/0.9 + [HCO_3^-]/4$$

$$TDS_{carb-H2CO3+H2SO4} = [Ca^{2+}]/1.1 + [Mg^{2+}]/0.9 + [HCO_3^-]/3.5.$$

Similarly, the CO_2 consumption rate of carbonate dissolution by only carbonic acid and by both sulfuric and carbonic acid can be calculated using the following equations, respectively:

$$CO_{2-H2CO3} = [HCO_3^-]/2$$

$$CO_{2-H2CO3+H2SO4} = [HCO_3^-]*3.5/1.5.$$

The calculated results show that the involvement of sulfuric acid in carbonate weathering resulted in an increase of around 6.5% in weathering rates, and a 13.8% decrease in CO_2 consumption rates. These results are comparable to those found in the studies of Wujiang River (Han and Liu, 2004), and Nanpanjiang and Beibanjiang River (Xu and Liu, 2007), in which the sulfuric acid resulted in a decrease of 10%, 9.2%, 17.5% in the CO_2 consumption by carbonate weathering by H_2CO_3, respectively. However, the result found here is lower than that of the Baishuijiang River, in which 60% of sulfate in the river is derived from oxidative weathering of sulfide minerals in sedimentary rocks (Li *et al.*, 2008).

Atmospheric inputs of sulfate to stream water and their impaction The stream water collected had Cl^- concentrations ranging from 15.4 to 117.3 μeq/L, with a mean of 36.9 μeq/L. Chloride typically has two main origins: atmospheric input and the dissolution of rock salt. However, there is no geological evidence for the presence of evaporates in the present catchment. As described earlier, the rainwater of the study area has an average Cl^- of 18.1 μeq/L, which is close to the minimum Cl^- in the stream. According to Han and Jin (1996), the evapotranspiration factor near the study region varies from 2 to 5. Therefore, the highest Cl^- concentration expected to originate from atmospheric inputs, delivered by rainwater can be estimated to have a critical value of around 36.2–90.5 μeq/L, of which the lower value is much closer to the mean observed Cl^- in the stream. Thus, we assume that the concentration of atmospheric-derived Cl^- in the stream water was close to 36.2 μeq/l. Given the discussion above, we estimate the atmospheric contribution to sulfate in the stream water to be around 236.8 μeq/L, accounting for around 73.9% of the total SO_4^{2-} in the stream water. As estimated earlier, around 94.3% of the sulfates in the deposition were derived from anthropogenic sources, in particular coal combustion. Thus, 69.7% of stream sulfate can be supposed to originate from sulfuric acid generated by coal combustion. We further estimate that these atmospheric anthropogenic sources of sulfate can cause a decrease of around 9.6% in the CO_2 consumption rates in the study area. Although the precise extent to which the atmospheric sulfuric acid derived mainly from anthropogenic sources contributes to the rock weathering should be further clarified, in view of the regional and global budget of CO_2, the data available at present indicate that even in the rural karst region of southwest China, the involvement of anthropogenic sulfate can significantly decrease the carbon uptake rate by carbonate weathering.

Summary and Conclusions

(1) The Huanjiang rainwater exhibited a VWM pH of 5.1, and sulfate was the major acidifying ion, ranging from 36.4 to 585.6 μeq/L, with a mean of 181.0 μeq/L. Ca^{2+} is the most abundant cation, ranging from 21.9 to 219.6 μeq/L with a mean value of 102.5 μeq/L. NH_4^+ is the second most abundant cation in the rainwater samples, with concentrations varying from 3.0 to 396.2 μeq/L, with a mean

value of 86.3 μeq/L.

(2) The seasonal variations in ionic deposition fluxes were not consistent with the ionic concentrations. Although the VWM concentrations of TZ followed a sequence of autumn > winter > spring > summer, the highest wet deposition of ions is observed in the summer, as a result of the higher rainfall quantities and higher frequency of rain events, with the exception of SO_4^{2-} and NH_4^+, which have their highest fluxes in spring.

(3) Statistical analysis indicated that the predominant species combinations of rainwater were NaCl, $CaSO_4$, $MgSO_4$, $(NH_4)_2SO_4$, K_2SO_4, NH_4NO_3, $Ca(NO_3)_2$, and $Mg(NO_3)_2$, which may form within atmospheric water droplets by aerosol scavenging and by subsequent reaction of gaseous species on the aerosol.

(4) The statistical analysis and enrichment factor study showed that the main sources of Na^+ and Cl^- were sea salt, and of Ca^{2+} and Mg^{2+} were the Earth's crust, accounting for 99.0% and 89.9% of their total content in the rain, respectively. Meanwhile, SO_4^{2-} and NO_3^- were derived from anthropogenic sources, accounting for 94.3% and 98.3% of their total amount, respectively. The $\delta^{34}S$–SO_4^{2-} of the rain ranged from –5.6~–11.0‰, with a mean value of –8.4‰, which points towards the combustion of local coal as the main source of sulfate in the rainwater.

(5) The precipitation events classified by their air-mass back-trajectories showed that the anthropogenic sources of SO_4^{2-} and NO_3^- might be affected by air mass origin and passes. It is notable that the only city within 50 km from study site contributed atmosphere pollutants with different SO_4^{2-}/NO_3^- ratios, and Liuzhou city, one of the most important heavy industry cities in China, which is located around 190 km away from the study site may be an important factor controlling the SO_4^{2-} and NO_3^- content of the rainwater. This was further supported by the $\delta^{34}S$–SO_4^{2-} of non-sea salt sources of ions in the rain.

(6) The involvement of sulfuric acid in carbonate weathering at the study site resulted in around a 6.5% increase in weathering rates, but a 13.8% decrease of the CO_2 consumption rates. We further estimated that atmospheric sulfate, mainly from coal combustion, can cause a decrease of up to 9.6% in the CO_2 consumption rates in the study area. The data available at present indicate that even in the rural karst regions of southwest China, the involvement of anthropogenically derived sulfate can significantly decrease the carbon uptake rate of carbonate weathering.

Acknowledgments—This work was jointly financially supported by the 973 Program (No. 2013CB956700), and the Chinese National Natural Science Foundation (Nos. 41203090, 41073099 and 41021062). Many thanks go to Dr. Jing Zhang for her helpful insights, which contributed to significant improvement of the manuscript, and Mr. Tze Hung Seeto for improvement in English writing. We thank An-Gui Meng, Hai-Tao Li, and Wen-Jing Liu for their help in fieldwork and sample analysis.

REFERENCES

Aas, W., Shao, M., Jin, L., Larssen, T., Zhao, D., Xiang, R., Zhang, J., Xiao, J. and Duan, L. (2007) Air concentrations and wet deposition of major inorganic ions at five non-urban sites in China, 2001–2003. *Atmos. Environ.* **41**, 1706–1716.

Bricker, O. P. and Rice, K. C. (1993) Acid-rain. *Annu. Rev. Earth Planet. Sci.* **21**, 151–174.

Charlson, R. J. and Rodhe, H. (1982) Factors controlling the acidity of natural rainwater. *Nature* **295**, 683–685.

Dibb, J. E., Talbot, R. W., Whitlow, S. I., Shipham, M. C., Winterle, J., McConnell, J. and Bales, R. (1996) Biomass burning signatures in the atmosphere and snow at Summit, Greenland: An event on 5 August 1994. *Atmos. Environ.* **30**, 553–561.

Ding, H. (2010) Water and nutrient cycle of typical Karst Peak-Cluster Depression: a case study in Mulian Catchment, NW of Guangxi Province, China. Dr. Sci. Thesis, Inst. Geochem., 220 pp. (in Chinese).

Galloway, J. N. (1995) Acid deposition: Perspectives in time and space. *Water, Air, and Soil Pollut.* **85**, 15–24.

Han, G. and Liu, C.-Q. (2004) Water geochemistry controlled by carbonate dissolution: a study of the river waters draining karst-dominated terrain, Guizhou Province, China. *Chem. Geol.* **204**, 1–21.

Han, G. and Liu, C.-Q. (2006) Strontium isotope and major ion chemistry of the rainwaters from Guiyang, Guizhou Province, China. *Sci. Total Environ.* **364**, 165–174.

Han, G., Tang, Y., Wu, Q. and Tan, Q. (2010) Chemical and strontium isotope characterization of rainwater in karst virgin forest, Southwest China. *Atmos. Environ.* **44**, 174–181.

Han, Z. and Jin, Z. (1996) *Hydrology of Guizhou Province, China*. Seismology Press, Beijing.

Hao, J., Duan, L., Zhou, X. and Fu, L. (2001) Application of a LRT model to acid rain control in China. *Environ. Sci. Technol.* **35**, 3407–3415.

Hechi City Government (2010) *Hechi Statistical Yearbook 2009* (in Chinese).

Huang, D.-Y., Xu, Y.-G., Peng, P. A., Zhang, H.-H. and Lan, J.-B. (2009) Chemical composition and seasonal variation of acid deposition in Guangzhou, South China: Comparison with precipitation in other major Chinese cities. *Environ. Pollut.* **157**, 35–41.

Huang, K., Zhuang, G., Xu, C., Wang, Y. and Tang, A. (2008) The chemistry of the severe acidic precipitation in Shanghai, China. *Atmos. Res.* **89**, 149–160.

IMPACTS (2004) Integrated monitoring program on acidification of Chinese terrestrial systems. Annual Report, results 2003. NIVA Report No. 4905-2004, ISBN:4982-4577-4594-4904.

Ito, M., Mitchell, M. J. and Driscoll, C. T. (2002) Spatial patterns of precipitation quantity and chemistry and air temperature in the Adirondack region of New York. *Atmos. Environ.* **36**, 1051–1062.

Keene, W. C., Pszenny, A. A. P., Galloway, J. N. and Hawley,

M. E. (1986) Sea-salt corrections and interpretation of constituent ratios in marine precipitation. *J. Geophys. Res.* **91**, 6647–6658.

Larssen, T., Lydersen, E., Tang, D., He, Y., Gao, J., Liu, H., Duan, L., Seip, H. M., Vogt, R. D., Mulder, J., Shao, M., Wang, Y., Shang, H., Zhang, X., Solberg, S., Aas, W., Okland, T., Eilertsen, O., Angell, V., Li, O., Zhao, D., Xiang, R., Xiao, J. and Luo, J. (2006) Acid rain in China. *Environ. Sci. Technol.* **40**, 418–425.

Lei, H.-C., Tanner, P. A., Huang, M.-Y., Shen, Z.-L. and Wu, Y.-X. (1997) The acidification process under the cloud in southwest China: Observation results and simulation. *Atmos. Environ.* **31**, 851–861.

Li, S.-L., Calmels, D., Han, G., Gaillardet, J. and Liu, C.-Q. (2008) Sulfuric acid as an agent of carbonate weathering constrained by δ13CDIC: Examples from Southwest China. *Earth Planet. Sci. Lett.* **270**, 189–199.

Li, Y., Yu, X., Cheng, H., Lin, W., Tang, J. and Wang, S. (2010) Chemical characteristics of precipitation at three Chinese regional background stations from 2006 to 2007. *Atmos. Res.* **96**, 173–183.

Liu, C. Q. (2007) *Biogeochemical Processes and Cycling of the Nutrients in the Earth's Surface—Chemical Erosion and Nutrient Cycling in Karstic Catchment, Southwest China*. Science Press, Beijing. 889 pp. (in Chinese).

Mizoguchi, T., Zhang, J., Satake, H., Mukai, H., Murano, K. and Kawasaki, K. (2012) Lead and sulfur isotopic ratios in precipitation and their relations to trans-boundary atmospheric pollution. *Atmos. Res.* **104**, 237–244.

Mukai, H., Tanaka, A., Fujii, T., Zeng, Y., Hong, Y., Tang, J., Guo, S., Xue, H., Sun, Z., Zhou, J., Xue, D., Zhao, J., Zhai, G., Gu, J. and Zhai, P. (2001) Regional characteristics of sulfur and lead isotope ratios in the atmosphere at several Chinese urban sites. *Environ. Sci. Technol.* **35**, 1064–1071.

Négrel, P. and Roy, S. (1998) Chemistry of rainwater in the Massif Central (France): a strontium isotope and major element study. *Appl. Geochem.* **13**, 941–952.

Okuda, T., Iwase, T., Ueda, H., Suda, Y., Tanaka, S., Dokiya, Y., Fushimi, K. and Hosoe, M. (2005) Long-term trend of chemical constituents in precipitation in Tokyo metropolitan area, Japan, from 1990 to 2002. *Sci. Total Environ.* **339**, 127–141.

Pena, J. A., de Pena, R. G., Bowersox, V. C. and Takacs, J. F. (1982) SO_2 content in precipitation and its relationship with surface concentrations of SO_2 in the air. *Atmos. Environ. (1967)* **16**, 1711–1715.

Qin, L., Huang, K., Wang, J., Zhao, C. and Luo, J. (2011) Characteristics and tendency of acid rain in Hechi City during 2005 to 2010. *J. Guanxi Acad. Sci.* **27**, 102–104 (in Chinese).

Reimann, C. and Caritat, P. D. (2000) Intrinsic Flaws of Element Enrichment Factors (EFs) in environmental geochemistry. *Environ. Sci. Technol.* **34**, 5084–5091.

Rolph, G. D. (2011) *Real-time Environmental Applications and Display sYstem (READY)*. NOAA Air Resources Laboratory, Silver Spring, MD. Website http://ready.arl.noaa.gov

State Environmental Protection Administration of China (2008) *China Environmental Statement of 2007*. Beijing (in Chinese).

Tang, J., Xue, H., Yu, X., Cheng, H., Xu, X., Zhang, X. and Ji, J. (2000) The preliminary study on chemical characteristics of precipitation at Mt. Waliguan. *Acta Scientiae Circumstantiae* **20**, 420–425.

Tang, Y. (2011) Natural and anthropologic characteristcs of atmospheric dust in North and South China: Case study in semiarid and karst regions. Dr. Sci. Thesis, Inst. Geochem., 128 pp. (in Chinese).

Taylor, S. R. (1964) Abundance of chemical elements in the continental crust: a new table. *Geochim. Cosmochim. Acta* **28**, 1273–1285.

Toyama, K., Satake, H., Takashima, S., Matsuda, T., Tsuruta, M. and Kaeada, K. (2007) Long-range transportation of contaminants fromThe Asian Continent to The Northern Japan Alps, recorded in snow cover on Mt. Nishi-Hodaka-Dake. *Bull. Glaciological Res.* **24**, 37–47.

Wu, Q., Han, G., Tao, F. and Tang, Y. (2012) Chemical composition of rainwater in a karstic agricultural area, Southwest China: The impact of urbanization. *Atmos. Res.* **111**, 71–78.

Xiao, H. Y. and Liu, C. Q. (2002) Sources of nitrogen and sulfur in wet deposition at Guiyang, southwest China. *Atmos. Environ.* **36**, 5121–5130.

Xiao, H.-Y., Tang, C.-G., Xiao, H.-W., Liu, X.-Y. and Liu, C.-Q. (2010) Stable sulphur and nitrogen isotopes of the moss Haplocladium microphyllum at urban, rural and forested sites. *Atmos. Environ.* **44**, 4312–4317.

Xu, Z. and Han, G. (2009) Chemical and strontium isotope characterization of rainwater in Beijing, China. *Atmos. Environ.* **43**, 1954–1961.

Xu, Z. and Liu, C.-Q. (2007) Chemical weathering in the upper reaches of Xijiang River draining the Yunnan–Guizhou Plateau, Southwest China. *Chem. Geol.* **239**, 83–95.

Xu, Z., Li, Y., Tang, Y. and Han, G. (2009) Chemical and strontium isotope characterization of rainwater at an urban site in Loess Plateau, Northwest China. *Atmos. Res.* **94**, 481–490.

Zhang, H., Hu, A., Lu, C. and Zhang, G. (2002) Sulfur isotopic composition of acid deposition in South China Regions and its environmental significance. *China Environ. Sci.* **22**, 165–169 (in Chinese).

Zhang, J. and Liu, C.-Q. (2004) Major and rare earth elements in rainwaters from Japan and East China sea—Natural and anthropogenic sources. *Chem. Geol.* **209**, 315–326.

Zhang, Y. L., Lee, X. Q. and Cao, F. (2011) Chemical characteristics and sources of organic acids in precipitation at a semi-urban site in Southwest China. *Atmos. Environ.* **45**, 413–419.

Zhao, Z.-Q. and Liu, C.-Q. (2010) Anthropogenic inputs of boron into urban atmosphere: Evidence from boron isotopes of precipitations in Guiyang City, China. *Atmos. Environ.* **44**, 4165–4171.